

Three Level Four Leg Shunt Active Power Filter Based a New Three Dimensional Space Vector Modulation strategy in the $\alpha\beta 0$ -axes

Ali Chebabhi
ICEPS Laboratory
Department of Electrical
Engineering
University of Sidi Bel-
Abbes Algeria
chebabhiali@gmail.com

Mohammed K. Fellah
ICEPS Laboratory
Department of Electrical
Engineering
University of Sidi Bel-
Abbes Algeria
mkfellah@yahoo.fr

Mohamed F. Benkhoris
IREENA Laboratory
University of Nantes at
Saint Nazaire
France
Mohamed-
Fouad.Benkhoris@univ-
nantes.fr

Abdelhalim Kessal
Faculty of Science and
Technology
University of Bordj Bou
Arreridj
Algeria
abdelhalim.kessal@yahoo.fr

Abstract—This paper presents a new Three level Three Dimensional Space Vector Modulation (Three level 3D-SVM) strategy for three level four leg Neutral Point Clamped (NPC) inverter controlling which is competent to operate in Shunt Active Power Filter (SAPF), in order to reducing the source harmonic currents and the inverter harmonic output voltages, eliminating the zero-sequence current caused by single-phase non-linear loads, reducing the switching frequency and voltage supported by the switches, and to compensate the reactive power. Simulation results of three level four leg Shunt Active Power Filter performances are presented to validate the proposed three level 3D-SVM strategy for switching signals generating.

Keywords—Three level four leg SAPF, Three Level Three Dimensional Space Vector Modulation (Three-Level 3D-SVM), $pq0$ Theory; Zero-sequence current; Harmonic currents compensation; Reactive power compensation, PI.

I. INTRODUCTION

The four leg shunt active power filters (SAPFs) have extensively studied and effectively solution for improve the largely power factor by the compensation of harmonic currents , reactive power and zero sequence current elimination in three phase four wire electrical networks caused by three single-phase non-linear loads [1-3]. The four leg shunt active power filters commonly based on an four leg inverter for injects harmonics and zero sequence current in the electrical network, equal to that given by single phase non-linear loads, but in phase opposition there with into the point of common coupling (PCC) [4,5]. The four leg shunt active power filters are individual widely used on gained large of their capability to compensate for harmonics, zero sequence current and reactive power simultaneously in four wire network [5–7].

Conventional two-level four leg inverter configurations used as shunt active power filters are simply appropriate for low to medium power applications. However, multilevel inverter configurations are appropriate for high voltage, and medium to high power applications [8]. Three level three or four leg Neutral Point Clamped (NPC) inverters are now suitable exceptionally accepted for high power applications such as static var compensation, motor drives, and active

power filters [9–14], due to their advantages over the conventional two level inverters as they result in high voltage capability, almost sinusoidal output voltage and power quality associated with reduced harmonic distortion, lower electromagnetic interference (EMI) [22]. They can increase output voltage magnitude and reduce output voltage harmonic, switching frequency and voltage supported by each switch, and elevated competence than two level four leg inverter for active power filters and high power compensation applications [11]. Also the output voltage forms and the switching losses depends on the technique used for the switching signals generating of three level four leg Neutral Point Clamped (NPC) inverters controller.

Several strategies for switching signals generating to an multi-level four leg Neutral Point Clamped (NPC) SAPF with have been shown in the literature, such as the generation of switching signals by hysteresis [16,17], and by PWM [17, 18]. In this study, we use a new strategy called three level three Dimensional space vector modulation in the $\alpha\beta 0$ -axes (Three level 3D-SVM). Three level 3D-SVM ensures precise control with reduced harmonic distortion and constant the switching frequency compared to those obtained by hysteresis and PWM. Also this strategy not only inherits the fixation of switching frequency of inverter switches, but also improves the output voltage forms and provides a good dynamic response in the three level four leg inverter.

In this paper, to validate the correctness of the proposed new three level 3D-SVM strategy used for controlling the three level four leg Neutral Point Clamped (NPC) SAPF, the simulation of SAPF described previously was effected using Sim Power Systems and S-Function of MATLAB/SIMULINK. The objective of simulation is to study two different aspects: 1) The considerable decrease in shunt active power filter evaluation in comparison with Two-levels four leg SAPF controlled by two level 3D-SVM strategy proposed in [7] due to Three level four leg SAPF controlled by new three-level 3D-SVM strategy. 2) The reducing of output voltage harmonics, compensation of harmonics and reactive power, zero sequence current

eliminating and switching frequency reducing under loads variations.

II. MODELING OF THE THREE LEVEL FOUR LEG SHUNT ACTIVE POWER FILTER

The three level four leg shunt active power filter topology presented in this paper is shown in Fig. 1.

The main circuit contains a three phase non-linear load composed of three single phase Rectifier Bridge followed by R_{ch} and L_{ch} load, connected to a three phase source in a point called Point of Common Coupling (PCC).

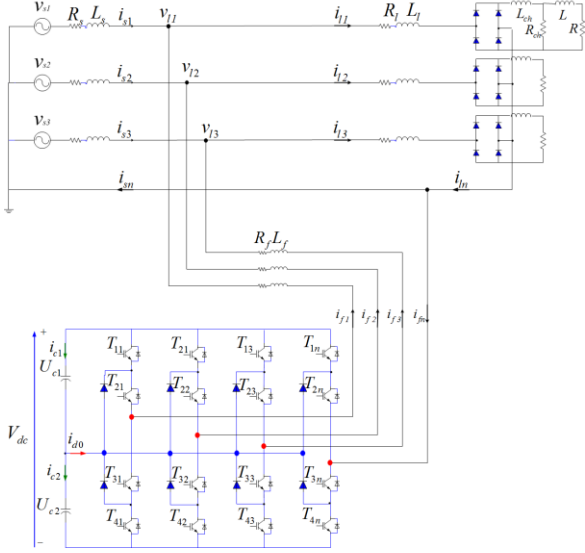


Fig. 1. Three level four leg shunt active power filter topology

A. Three level four leg inverter modulation

As in the two level four leg inverter [20], each switch of three level four leg inverter T_{ij} , $i, j \in \{1, 2, 3, 4\}$ operates two by two complementary more precisely by the switching function as follows:

$$F_j = \begin{cases} 1 & \text{if } T_{1j} \text{ and } T_{2j} \text{ is closed} \\ 0 & \text{if } T_{2j} \text{ and } T_{3j} \text{ is closed} \\ -1 & \text{if } T_{3j} \text{ and } T_{4j} \text{ is closed} \end{cases} \quad (1)$$

The operation two by two complementary switches is the following:

$$F_{ij} = 1 - F_{(i-2)j}, \quad i = 3, 4; j = 1, 2, 3, 4 \quad (2)$$

The three states of each leg F_j corresponding to the three switching functions F_{ij} is defined in the next way

$$F_j = \begin{cases} P & \text{if } F_{ij} = 1 \\ O & \text{if } F_{ij} = 0 \\ N & \text{if } F_{ij} = -1 \end{cases} \quad (3)$$

The three level four leg inverter Fig. 4 delivers at the output three level voltages, these voltages are expressed in terms of the DC bus capacitors voltages $V_{dc}/2$, 0, and $-V_{dc}/2$, and according to three possible states **PON** switches of each leg [12, 13] as follows:

State P: The upper two switches T_{1j} and T_{2j} are closed, while the two lower switches T_{3j} and T_{4j} are open. The output voltage is $v_j = V_{dc}/2$

State O: The middle two switches T_{2j} and T_{3j} are closed, while the two switches of the extremities T_{1j} and T_{4j} are open. The output voltage is $v_j = 0$

State N: The lower two switches T_{3j} and T_{4j} are closed, while the two upper switches T_{1j} and T_{2j} are open. The output voltage is $v_j = -V_{dc}/2$

The output voltages are expressed by: [12, 13], [15], [21]

$$v_{jo} = F_j \cdot \frac{V_{dc}}{2} \quad (4)$$

TABLE I. STATES OF ONLY LEG OF INVERTER

| States F_j of the leg j | States of i switches of the j leg | | | | Output voltage v_{jo} |
|-----------------------------|---------------------------------------|----------|----------|----------|-------------------------|
| | T_{1j} | T_{2j} | T_{3j} | T_{4j} | |
| P | 1 | 1 | 0 | 0 | $V_{dc}/2$ |
| O | 0 | 1 | 1 | 0 | 0 |
| N | 0 | 0 | 1 | 1 | $-V_{dc}/2$ |

v_{jo} is the output voltage of each leg. The output phase to neutral voltage is defined as:

$$v_{jn} = v_{jo} - v_{no} \quad (5)$$

Where v_{jo} is the voltage of the phase-middle imaginary point o, V_{dc} is the total DC bus voltage. Each leg of inverter can take three states (PON). Thus the three level four leg inverter is $3^4=81$ possible states. Table 2 summarizes the states of three level four leg inverter for each switching vector:

TABLE II. THE STATES OF THREE LEVEL FOUR LEGS INVERTER FOR EACH SWITCHING VECTOR

| v_i | States | v_i | States | v_i | States |
|----------|--------|----------|--------|----------|--------|
| v_1 | NNNN | v_{28} | ONNN | v_{55} | PNNN |
| v_2 | NNNO | v_{29} | ONNO | v_{56} | PNNO |
| v_3 | NNNP | v_{30} | ONNP | v_{57} | PNNP |
| v_4 | NNON | v_{31} | ONON | v_{58} | PNON |
| v_5 | NNOO | v_{32} | ONOO | v_{59} | PNOO |
| v_6 | NNOP | v_{33} | ONOP | v_{60} | PNOP |
| v_7 | NNPN | v_{34} | ONPN | v_{61} | PNPN |
| v_8 | NNPO | v_{35} | ONPO | v_{62} | POPO |
| v_9 | NNPP | v_{36} | ONPP | v_{63} | PNPP |
| v_{10} | NONN | v_{37} | OONN | v_{64} | PONN |
| v_{11} | NONO | v_{38} | OONO | v_{65} | PONO |
| v_{12} | NONP | v_{39} | OONP | v_{66} | PONP |
| v_{13} | NOON | v_{40} | OOON | v_{67} | POON |
| v_{14} | NOOO | v_{41} | OOOO | v_{68} | POOO |
| v_{15} | NOOP | v_{42} | OOPN | v_{69} | POPN |
| v_{16} | NOPN | v_{43} | OOPN | v_{70} | POPON |
| v_{17} | NOPO | v_{44} | OOPN | v_{71} | POPO |
| v_{18} | NOPP | v_{45} | OOPP | v_{72} | POPON |
| v_{19} | NPNN | v_{46} | OPNN | v_{73} | PPON |
| v_{20} | NPNO | v_{47} | OPNO | v_{74} | PPNO |
| v_{21} | NPNP | v_{48} | OPNP | v_{75} | PPPN |
| v_{22} | NPON | v_{49} | OPON | v_{76} | PPON |
| v_{23} | NPOO | v_{50} | OPOO | v_{77} | PPOO |
| v_{24} | NPOP | v_{51} | OPOP | v_{78} | PPOP |
| v_{25} | NPPN | v_{52} | OPPN | v_{79} | PPPN |
| v_{26} | NPPN | v_{53} | OPPN | v_{80} | PPPO |
| v_{27} | NPPP | v_{54} | OPPP | v_{81} | PPPP |

The differential equations describing the dynamic model of four-leg shunt active power filter in the $\alpha\beta$ -axes are defined, as given in equation (6): [7], [20]

$$\begin{cases} \frac{di_{f\alpha}}{dt} = -\frac{R_f}{L_f} i_{f\alpha} + \frac{1}{L_f} v_{f\alpha} - \frac{1}{L_f} v_{l\alpha} \\ \frac{di_{f\beta}}{dt} = -\frac{R_f}{L_f} i_{f\beta} + \frac{1}{L_f} v_{f\beta} - \frac{1}{L_f} v_{l\beta} \\ \frac{di_{f0}}{dt} = -\frac{R_f}{L_f} i_{f0} + \frac{1}{L_f} v_{f0} - \frac{1}{L_f} v_{l0} \\ \frac{dV_{dc}}{dt} = \frac{P_{dc}^*}{C V_{dc}} \end{cases} \quad (6)$$

III. THREE LEVEL THREE DIMENSIONAL SPACE VECTOR MODULATIONS

In 3D-SVM strategy in the three level four leg inverter, there are $3^4=81$ possible switching vectors: 79 active vectors and 3 null vectors. The Vector diagram of the three level four leg inverter is illustrated in Fig. 2.

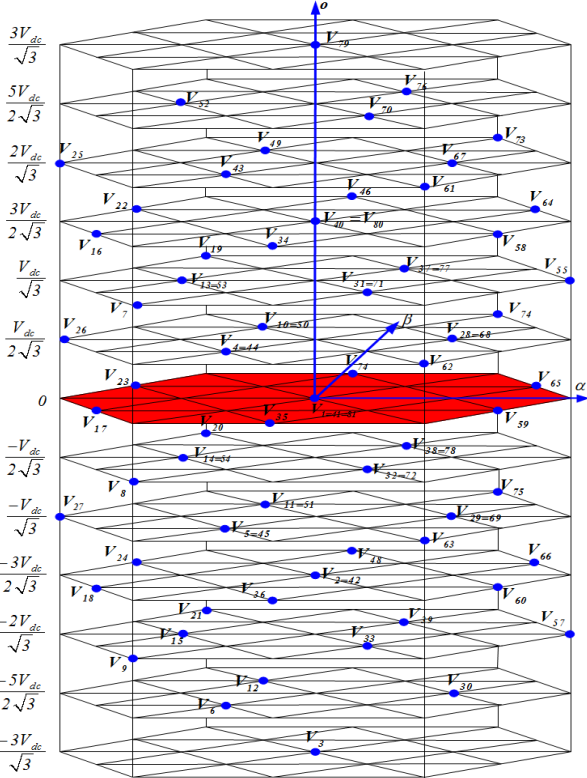


Fig. 2. The three level four leg inverter diagram vector

A. Prisms and sub-prisms identification

Such as the vector diagram of two level four leg inverter [1-2], [5], the vector diagram of three level four leg inverter is composed of six prisms Fig. 5 are labeled Prisms I through VI, each prism is decomposed into four sub-prism Fig. 5 are labeled SP₁-SP₄ and each sub-prism is decomposed into n tetrahedrons Fig. 5-7 and are summarized in Table 2.

To detect which sub-prism is the reference vector, it is necessary to determine the equation that defines the three sides of each sub-prism ($v_{f\alpha}^*, v_{f\beta}^*, v_{f0}^*$) coordinates in $\alpha\beta$ -axes. In this case, and to minimize the harmonics of the output voltage [13], is imposed on the voltage of the reference vector that locate inside the hexagon delimited by the outer circle Fig.5, which gives:

$$v_{loc} = \frac{\sqrt{3}}{2} V_{dc} \quad (7)$$

The four sub-prisms of each prism are deduced by using the equations of eight straight delimited (d_1, d_2, \dots, d_8 Fig. 6) that given as follows. [12]

$$\begin{cases} d_1 : v_{f\beta}^* = -\sqrt{3}v_{f\alpha}^* + \sqrt{\frac{1}{2}}V_{dc} \\ d_2 : v_{f\beta}^* = \sqrt{\frac{1}{8}}V_{dc} \\ d_3 : v_{f\beta}^* = \sqrt{3}v_{f\alpha}^* - \sqrt{\frac{1}{2}}V_{dc} \\ d_4 : v_{f\beta}^* = \sqrt{3}v_{f\alpha}^* \\ d_5 : v_{f\beta}^* = \sqrt{3}v_{f\alpha}^* + \sqrt{\frac{1}{2}}V_{dc} \\ d_6 : v_{f\beta}^* = -\sqrt{3}v_{f\alpha}^* \\ d_7 : v_{f\beta}^* = -\sqrt{3}v_{f\alpha}^* - \sqrt{\frac{1}{2}}V_{dc} \\ d_8 : v_{f\beta}^* = -\sqrt{\frac{1}{8}}V_{dc} \end{cases} \quad (8)$$

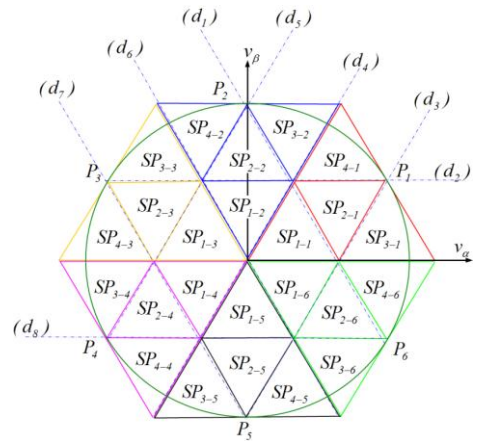
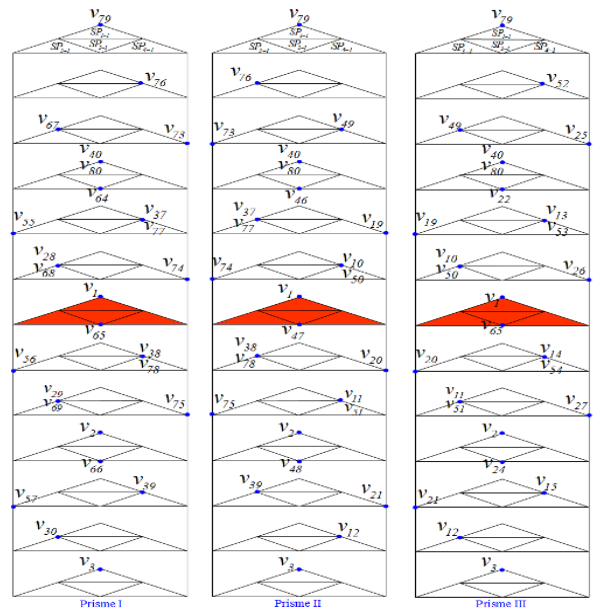


Fig. 3. Representation straight bounded sub-prism vector diagram of the three level four legs inverter.



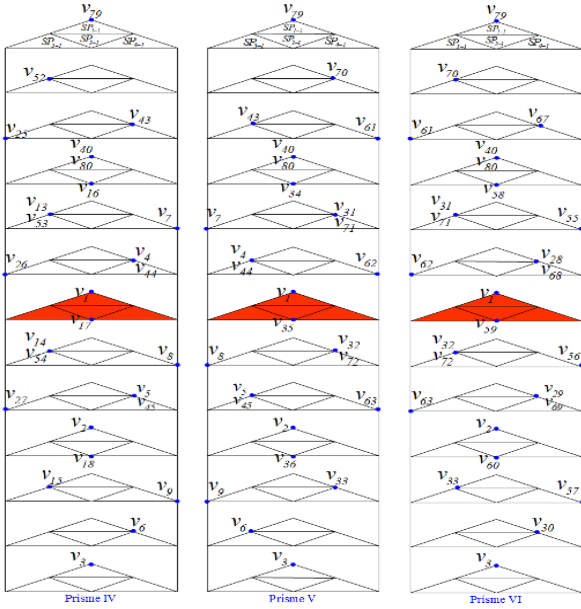


Fig. 4. Representation of sub-prisms in the vector diagram of three level four leg inverter

TABLE III. THE THREE LEVEL FOUR LEG INVERTER SWITCHING VECTORS FOR EACH SUB-PRISM

| P | SP | Switching Vectors |
|---|-------------------|---|
| 1 | SP ₁₋₁ | $v_{79}, v_{76}, v_{67}, v_{40}, v_{80}, v_{77}, v_{68}, v_1, v_{78}, v_{69}, v_2, v_{39}, v_{30}, v_3$ |
| | SP ₂₋₁ | $v_{67}, v_{64}, v_{55}, v_{68}, v_{65}, v_{56}, v_{69}, v_{66}, v_{57}, v_{30}$ |
| | SP ₃₋₁ | $v_{76}, v_{67}, v_{64}, v_{77}, v_{68}, v_{65}, v_{78}, v_{69}, v_{66}, v_{39}, v_{30}$ |
| | SP ₄₋₁ | $v_{76}, v_{73}, v_{64}, v_{77}, v_{74}, v_{65}, v_{78}, v_{75}, v_{66}, v_{39}$ |
| 2 | SP ₁₋₂ | $v_{79}, v_{76}, v_{49}, v_{40}, v_{77}, v_{10}, v_1, v_{78}, v_{11}, v_2, v_{39}, v_{12}, v_3$ |
| | SP ₂₋₂ | $v_{76}, v_{73}, v_{46}, v_{77}, v_{74}, v_{47}, v_{78}, v_{75}, v_{48}, v_{39}$ |
| | SP ₃₋₂ | $v_{76}, v_{49}, v_{46}, v_{77}, v_{10}, v_{47}, v_{78}, v_{11}, v_{48}, v_{39}, v_{12}$ |
| | SP ₄₋₂ | $v_{49}, v_{46}, v_{19}, v_{10}, v_{47}, v_{20}, v_{11}, v_{48}, v_{21}, v_{12}$ |
| 3 | SP ₁₋₃ | $v_{79}, v_{52}, v_{49}, v_{40}, v_{53}, v_{10}, v_1, v_{54}, v_{11}, v_2, v_{15}, v_{12}, v_3$ |
| | SP ₂₋₃ | $v_{49}, v_{22}, v_{19}, v_{10}, v_{23}, v_{20}, v_{11}, v_{24}, v_{21}, v_{12}$ |
| | SP ₃₋₃ | $v_{52}, v_{49}, v_{22}, v_{53}, v_{10}, v_{23}, v_{54}, v_{11}, v_{24}, v_{15}, v_{12}$ |
| | SP ₄₋₃ | $v_{52}, v_{25}, v_{22}, v_{53}, v_{26}, v_{23}, v_{54}, v_{27}, v_{24}, v_{15}$ |
| 4 | SP ₁₋₄ | $v_{79}, v_{52}, v_{43}, v_{40}, v_{53}, v_{44}, v_1, v_{54}, v_{45}, v_2, v_{15}, v_6, v_3$ |
| | SP ₂₋₄ | $v_{52}, v_{25}, v_{16}, v_{53}, v_{26}, v_{17}, v_{54}, v_{27}, v_{18}, v_{15}$ |
| | SP ₃₋₄ | $v_{52}, v_{43}, v_{16}, v_{53}, v_{44}, v_{17}, v_{54}, v_{45}, v_{18}, v_{15}, v_6$ |
| | SP ₄₋₄ | $v_{43}, v_{16}, v_7, v_{44}, v_{17}, v_8, v_{45}, v_{18}, v_9, v_6$ |
| 5 | SP ₁₋₅ | $v_{79}, v_{70}, v_{43}, v_{40}, v_{71}, v_{44}, v_1, v_{72}, v_{45}, v_2, v_{33}, v_6, v_3$ |
| | SP ₂₋₅ | $v_{43}, v_{34}, v_{71}, v_{44}, v_{35}, v_8, v_{45}, v_{36}, v_9, v_6$ |
| | SP ₃₋₅ | $v_{70}, v_{43}, v_{34}, v_{71}, v_{44}, v_{35}, v_{72}, v_{45}, v_{36}, v_{33}, v_6$ |
| | SP ₄₋₅ | $v_{70}, v_{61}, v_{34}, v_{71}, v_{62}, v_{35}, v_{72}, v_{63}, v_{36}, v_{33}$ |
| 6 | SP ₁₋₆ | $v_{79}, v_{70}, v_{67}, v_{40}, v_{71}, v_{68}, v_1, v_{72}, v_{69}, v_2, v_{33}, v_{30}, v_3$ |
| | SP ₂₋₆ | $v_{70}, v_{61}, v_{58}, v_{71}, v_{62}, v_{59}, v_{72}, v_{63}, v_{60}, v_{33}$ |
| | SP ₃₋₆ | $v_{70}, v_{67}, v_{58}, v_{71}, v_{68}, v_{59}, v_{72}, v_{69}, v_{60}, v_{33}, v_{30}$ |
| | SP ₄₋₆ | $v_{67}, v_{58}, v_{55}, v_{68}, v_{59}, v_{56}, v_{69}, v_{60}, v_{57}, v_{30}$ |

B. Tetrahedrons identification

The tetrahedron is formed by four switching vectors, as shown in Fig. 8, these figure describes the representation of tetrahedron 1 plans belonging to first sub-prism SP₁₋₁. [12]

For detecting at which tetrahedron is the reference vector \vec{v}_f^* , it is necessary to determine the equation defined the position of each tetrahedron in $\alpha\beta$ -axes. The first sub-prism of first prism is formed by ten tetrahedrons. For first sub-prism of first prism the tetrahedron T₁ is combines by four

switching vectors $\{v_{79}, v_{76}, v_{67}, v_{40}\}$, obeyed at the following position equation:

$$\begin{cases} a \cdot 0 + b \cdot 0 + c = \frac{3}{2\sqrt{3}} V_{dc} \rightarrow v_{40} \\ a \cdot \frac{V_{dc}}{\sqrt{6}} + b \cdot 0 + c = \frac{2}{\sqrt{3}} V_{dc} \rightarrow v_{67} \\ a \cdot \frac{V_{dc}}{\sqrt{24}} + b \cdot \frac{\sqrt{2}}{4} V_{dc} + c = \frac{5}{2\sqrt{3}} V_{dc} \rightarrow v_{76} \end{cases} \quad (9)$$

This gives:

$$a = \frac{\sqrt{2}}{2}, b = \sqrt{\frac{3}{2}}, c = \frac{3}{2\sqrt{3}} V_{dc} \quad (10)$$

The equation for detecting the position of first tetrahedron of first sub-prism of first prism is given by:

$$v_{f\alpha}^* > \frac{\sqrt{2}}{2} v_{f\alpha} + \sqrt{\frac{3}{2}} v_{f\beta} + \frac{3}{2\sqrt{3}} V_{dc} \quad (11)$$

Fig.7 describes the representation of equation that detected the position of the first tetrahedron in first sub-prism of the first prism (SP₁₋₁-T₁): The table 6 summarizes the four switching vectors of each tetrahedron for each sub-prism.

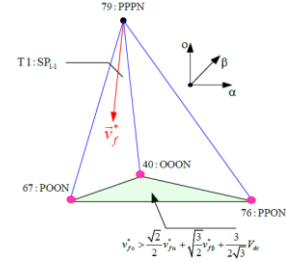


Fig. 5. Representation the position of first tetrahedron in the first sub-prism in the first prism (T1: SP1-1)

After that, the distributions of tetrahedrons in each sub-prism are shows in fig.6 and are given as follows:

- The sub-prism SP₁ content 10 tetrahedrons
- The sub-prism SP₂ content 8 tetrahedrons
- The sub-prisms SP₃ and SP₄ content 7 tetrahedrons

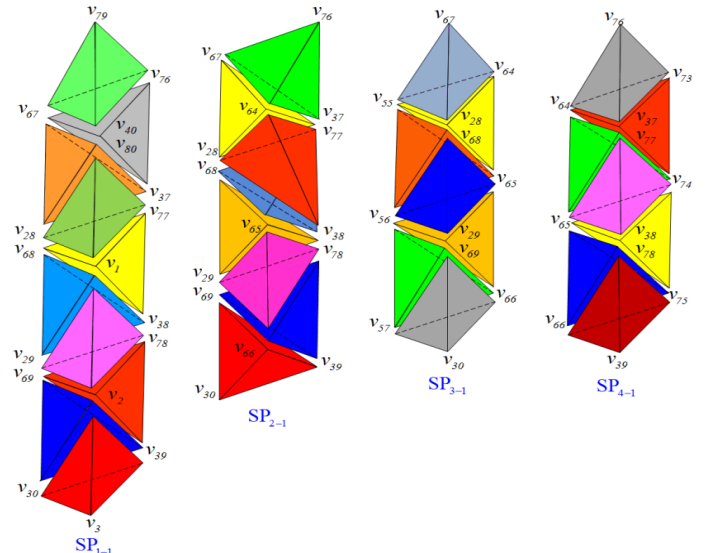


Fig. 6. Representation the distribution of tetrahedrons in each sub-prism

C. The time duration of the selected switching vectors

The principle of three level 3D-SVM is to project the desired switching vector on $\alpha\beta$ -axes, as shown in Fig. 5. We use these projections to calculate the switching time [7].

D. The Switching controls generation

The Fig. 6 shows the distribution of switching vectors to be applied in the $T_1:SP_{1-1}$ on a switching period.

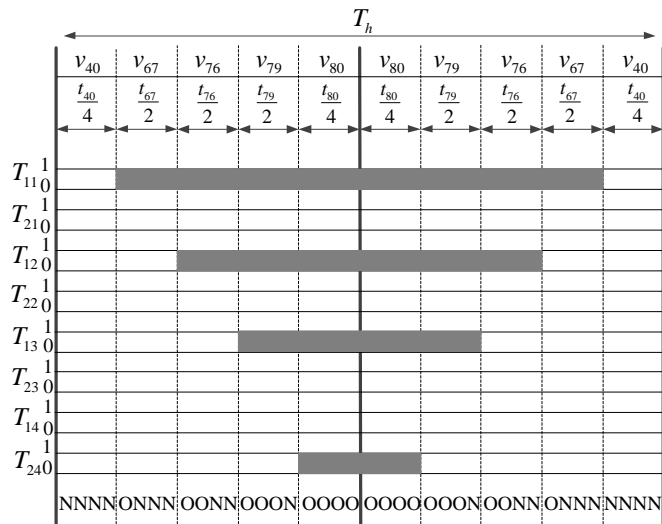


Fig. 7. Principle of switching signals generating by three level 3D-SVM

IV. SIMULATION CONTROL OF THE FOUR LEG SHUNT ACTIVE POWER FILTER

The work objective is to compare study of two different inverter topologies and their switches control uses in four leg SAPF. The inverter topologies and their switching signals generating that are considered for comparative study are: Two level four leg SAPF controlled by two level 3D-SVM proposed in [7] due to three level four leg SAPF controlled by new three level 3D-SVM. This is carried out by numerical simulation under the same conditions. The performance of the proposed control strategy is evaluated through Sim Power Systems and S-Function of MATLAB fig. 8.

The simulation results of the two topologies of four leg SAPF are given in Figs. (9-16), with the operating conditions: The DC voltage at the input of inverter is 800V, divided into two equal values, with two capacitors of $5 \cdot 10^{-3}$ Farads for each, and the sampling time T_e is equal 100 μs .

Figs 9 and 11 (a, b and c) represent the phase-to-neutral point output voltage v_{fln} and their analysis harmonics for the two topologies of four leg SAPF with the two types of switching signals generating (two level 3D-SVM and three level 3D-SVM) and with various values of Switching frequency (7, 10 and 14KHz), these figs shows that for same sampling time, the output voltage distortion harmonics THD are proportional with the Switching frequency.

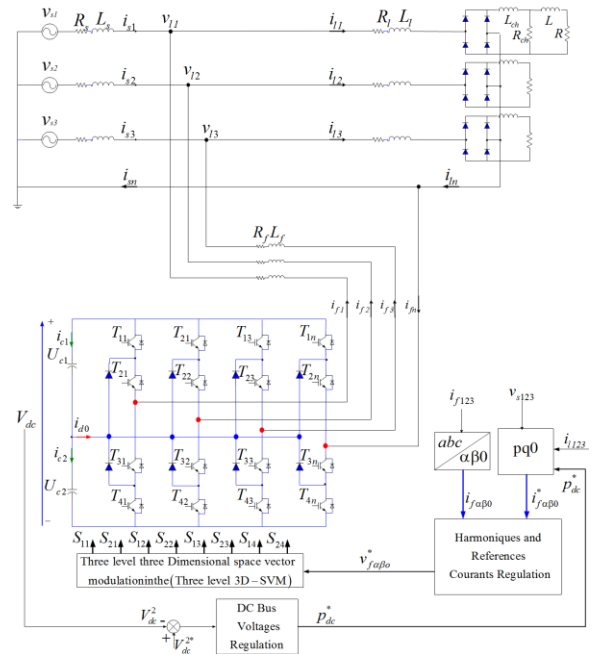


Fig. 8. Schematic block diagram of a control of three level four leg shunt active power filter

The distortion harmonics of output voltages for both four-leg shunt active power filter are approximately centered around the multiples of report N between the period of commutation T_s and the period of output voltage $T=0.02s$.

For the case of $f_s=7$ kHz, $T_s=1/7000s$ and $N=0.02 \cdot 7000$ thus $N=140$ period, figs 9 and 11-a.

For the case of $f_s=10$ kHz, $T_s=1/10000s$ and $N=0.02 \cdot 10000$ thus $N=200$ period, figs 9 and 11-b.

For the case of $f_s=14$ kHz, $T_s=1/14000s$ and $N=0.02 \cdot 14000$ thus $N=280$ period, figs 9 and 11-c.

According to output voltages harmonics distortion (THD_v) obtained for both four-leg shunt active power filter with the two types of switching signals generating under same switching frequency, it can be found that the output voltages harmonics distortion for same switching frequency are minimum in three level four leg SAPF controlled by three level 3D SVM as compared to two level four leg SAPF controlled by two level 3D SVM. This three level four leg SAPF controlled by three level 3D SVM also presents high output voltage forms.

Figs 11 and 12 shows the switching signals of the two topologies of four-leg shunt active power filter (impulses of first switch of first leg) for various values of switching frequency. These figures show that, for same conductions of simulations, even sampling period, and the same values of switching frequency, the switching losses are arrangement reduced in the three level four leg shunt active power filter controlled by three level SVM 3D (figs 11) compared to two level four leg shunt active power filter controlled by SVM 3D (Figs 12) [7].

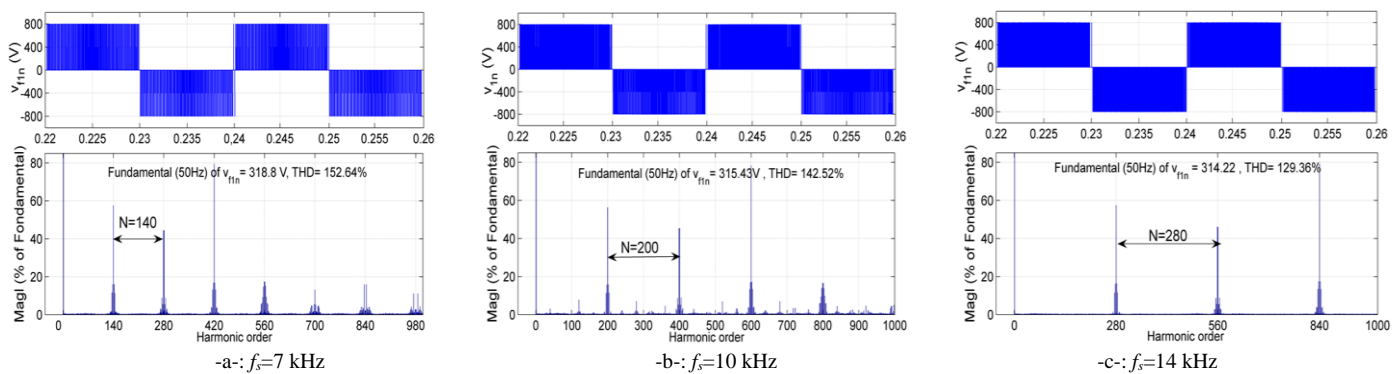


Fig. 9 Output voltages phase-to-neutral point v_{fln} and their THDv of two level four leg SAPF controlled by two level 3D SVM

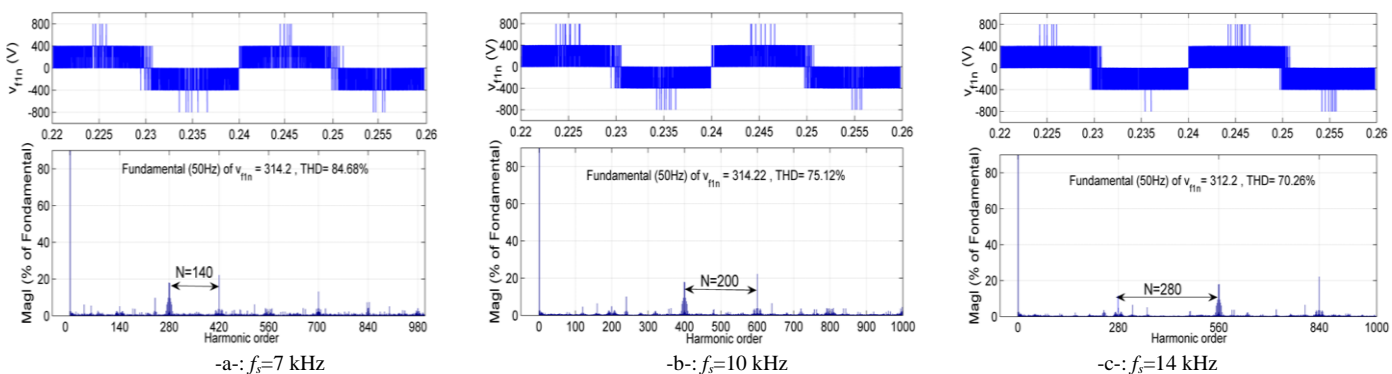


Fig. 10 Output voltage phase-to-neutral point voltage v_{fln} and their THDv of three level four leg SAPF controlled by three level 3D SVM

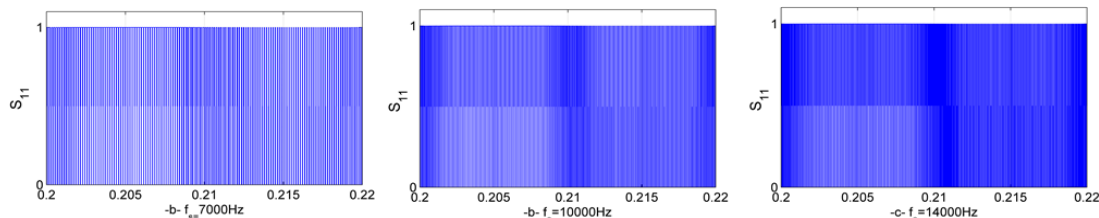


Fig.11 Switching pulses of first switch (T_1) of two level four leg SAPF controlled by two level 3D SVM

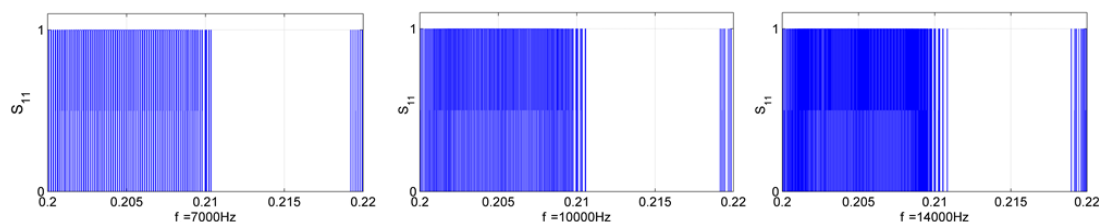


Fig.12 Switching pulses of first switch (T_1) of three level four leg SAPF controlled by three level 3D SVM

Figs. 13 and 14 (a, b and c) demonstrate the four leg shunt active power filter performance with the two topologies of four leg SAPF and their two types of switching signals generating under different loads conditions, the source currents waveform are sinusoidal and the neutral wire current is successfully reduced for all cases and various values of switching frequency, as well as smaller magnitudes than in the three level four leg SAPF controlled by three level 3D SVM. For both four leg SAPF with the two types of switching signals generating, the reactive power in the source is almost zero, which means also that the source has a power factor almost of unity before and after unbalanced loads, as well as

smaller undulations than in the three level four leg SAPF controlled by three level 3D SVM.

The first phase source current spectra before and after unbalanced loads with various values of Switching frequency are given in Fig.15 and 16 (a, b and c) for both two level four leg SAPF controlled by two level 3D SVM [7] and three level four leg SAPF controlled by three level 3D SVM schemes are well below; the limit imposed by the IEEE-519 or CEI 61000 standards, and the total harmonics distortion for all various values and in same values of switching frequency are more lowest in the three level four leg SAPF controlled by three level 3D SVM compared to the two level four leg SAPF controlled by 3D SVM [7].

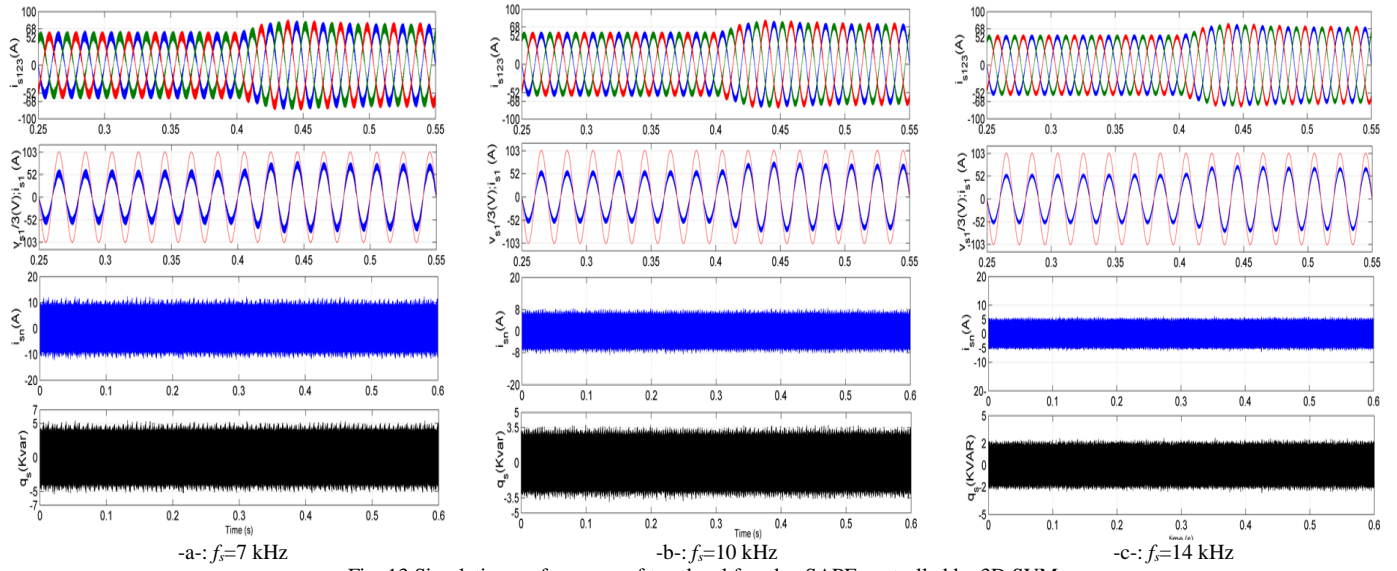


Fig. 13 Simulation performance of two level four leg SAPF controlled by 3D SVM

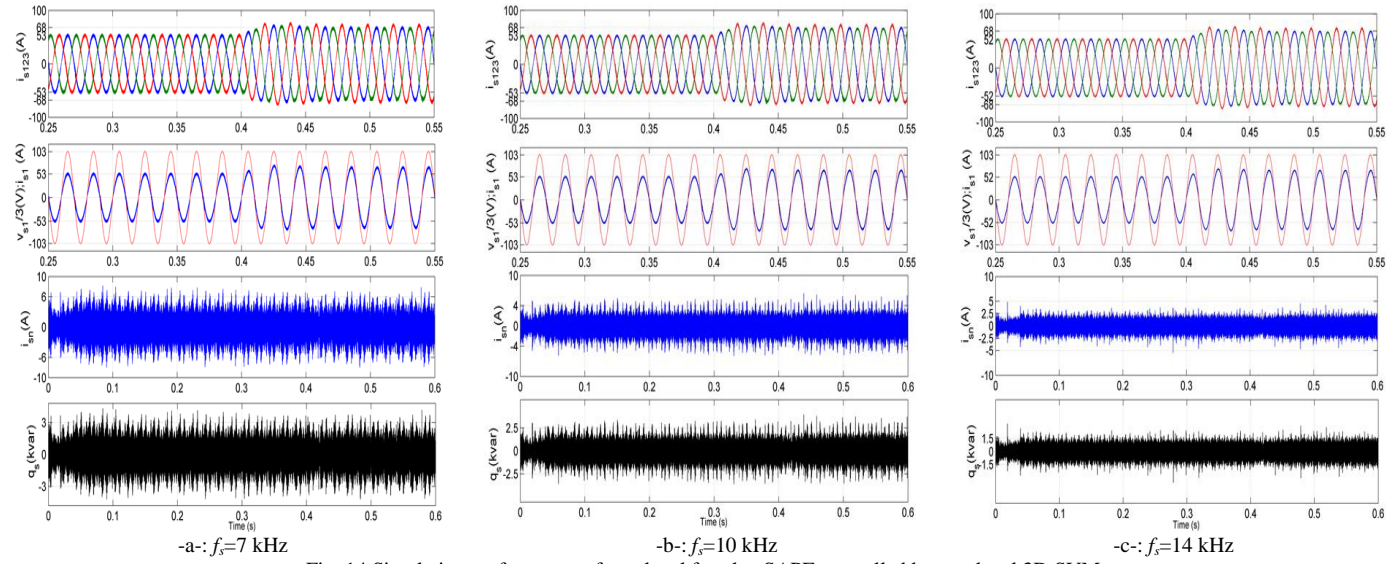


Fig. 14 Simulation performance of two level four leg SAPF controlled by two level 3D SVM

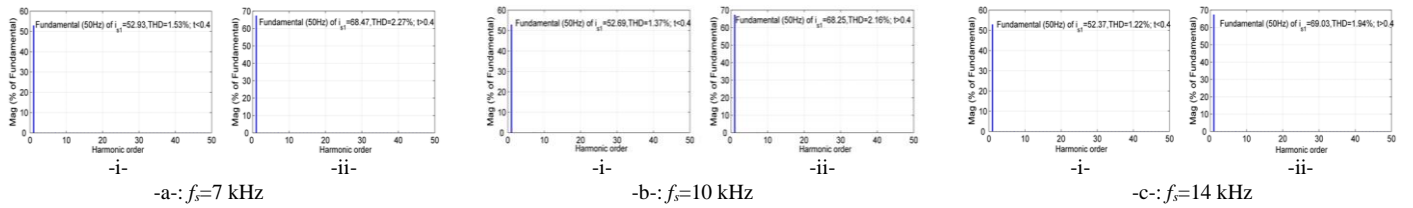


Fig. 15 Spectrum of source current for two level four leg SAPF controlled by two level 3D SVM: (i) before unbalanced loads, (ii) after unbalanced loads

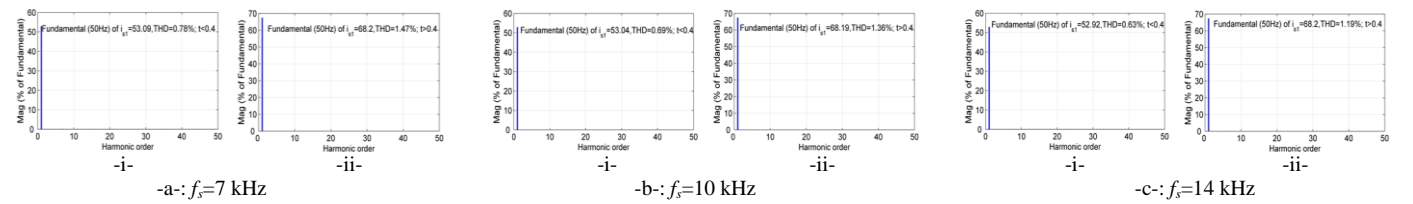


Fig. 16 Spectrum of source current for three level four leg SAPF controlled by three level 3D SVM: (i) before unbalanced loads, (ii) after unbalanced loads

V. CONCLUSION

In this work theoretical study and verify with simulation of a shunt active power filter with three level four leg inverter NPC structure is proposed to improve the power quality under unbalanced loads. And a new three level Three Dimensional Space Vector Modulation (Three level 3D-SVM) control strategy was presented for switching signals generating of the three level four leg inverter. This control strategy

accomplished to reduce the switching losses, fixed switching frequency and to improve the inverter output voltages forms over the conventional control strategies. The simulation results of three level four leg SAPF controlled by three level 3D SVM also shows better dynamic performances over the two level four leg SAPF controlled by 3D SVM. The following objectives have been successfully carried even with three level four leg SAPF controlled by three level 3D SVM under unbalanced loads:

- 1) Harmonics and zero-sequence current filtering and minimizing.
- 2) Switching losses reducing, and fixed switching frequency of inverter switches.
- 3) Neutral wire current magnitude and reactive power undulations reducing's.
- 4) Reactive power compensation.
- 5) The inverter output voltages forms improved.

ACKNOWLEDGMENTS

The authors like to thank the ICEPS Laboratory (Djillali Liabès University of Sidi Bel-Abbes) and the Algerian general direction of research DGRDT for their financial support.

REFERENCES

- [1] A. Chebabhi, M-K Fellah, A. Kessal, M-F Benkhoris «Comparative Study of reference currents and DC bus voltage Control for Three Phase Four Wire Four Leg shunt active power filter to Compensate Harmonics and Reactive Power with 3D SVM», ISA Transactions 02/2015; DOI:10.1016/j.isatra.2015.
- [2] A. Chebabhi, M-K Fellah, M-F Benkhoris «Control of the Three Phase four-wire four-leg SAPF Using 3D-SVM Based on the Two Methods of Reference Signals Generating CV and SRF in the dq0-axes», Journal of Electrical Engineering 03/2015; 1(1):32-39.
- [3] A. S. Abu Hasim, M. H. N. Talib, Z. Ibrahim «Comparative Study of Different PWM Control Scheme for Three-Phase Three -Wire Shunt Active Power Filter », IEEE International Power Engineering and Optimization Conference (PEDCO) Melaka,Malaysia, 2012.
- [4] I. I. Abdalla, K. S. Rama Rao, N. Perumal, «Three-phase Four-Leg Shunt Active Power Filter to Compensate Harmonics and Reactive Power», IEEE Symposium on Computers & Informatics (ISCI), pp. 495 - 500, 2011.
- [5] H. Golwala, R. Chudamani, «Comparative Study of Switching Signal Generation Techniques for Three Phase Four Wire Shunt Active Power Filter», IEEE International Electric Machines & Drives Conference (IEMDC), pp: 1409–1414, 15-18 May, 2011.
- [6] H. Kouara, A. Chaghi «Three phase four wire shunt active power filter based fuzzy logic dc-bus voltage control», Acta Technica Corviniensis-Bulletin of Engineering, Tome V, 2012.
- [7] A. Chebabhi, M-K fellah, M-F Benkhoris «3D Space Vector Modulation Control of four-leg shunt active power filter using pq0 theory» Rev. Roum. Sci. Techn.– Électrotechn. et Énerg Bucarest, Vol:60 N° 2 Juin 2015, pp :185-194.
- [8] A. Benaissa, B. Rabhi, A. Moussi, M. F. Benkhoris, «Fuzzy logic controller for three-phase four-leg five-level shunt active power filter under unbalanced non-linear load and distorted voltage conditions», Int J Syst Assur Eng Manag, 2013.
- [9] E. Benyoussef, A. Meroufel, S. Barkat «Three-Level Direct Torque Control Based on Space Vector Modulation with Balancing Strategy of Double Star Synchronous Machine», Journal of Electrical Engineering Vol. 3 No. 3, 2013 PP. 25-30.
- [10] E. Benyoussef, A. Meroufel, S. Barkat «Three-Level Direct Torque Control Based on Space Vector Modulation with Balancing Strategy of Double Star Synchronous Machine», Journal of Electrical Engineering Vol. 3 No. 3, 2013 PP. 25-30.
- [11] T. Abdelkrim, K. Benamrane, B. Bezza, Aeh Benkhelifa, A. Borni «Three-Level Converters Back-to-Back DC Bus Control for Torque Ripple Reduction of Induction Motor», International Journal of Electrical, Electronic Science and Engineering Vol:8 No:5, 2014.
- [12] A. Chebabhi, M-K Fellah, M-F Benkhoris, A. Kessal «Fuzzy logic controllers and Three Dimensional Space Vector Modulation technique in the $\alpha\beta$ axes for three-phase four-wire four-leg shunt active power filter », The 2nd International Conference on Power Electronics and their Applications (ICPEA 2015), University of Djelfa, Algeria; 03/2015.
- [13] D.Lalili, E. M.Berkouk, F.Boudjema , Lourci N.,Taleb T. and Petzold, J., «Simplified space vector PWM algorithm for three-level inverter with neutral point potential control», The Mediterranean Journal of Measurement and Control, Vol.3, No. 1, January 2007, pp. 30-39.
- [14] S. Chennai «Three-level Neutral Point Clamped Shunt Active Power Filter performances using intelligent controllers», Rev. Roum. Sci. Techn.– Électrotechn. et Énerg, vol :59, no:3, pp: 303–313, 2014.
- [15] A. Benaissa, B. Rabhi, A. Moussi, M. F. Benkhoris, J.C. Le Claire «Fuzzy logic controller for five-level shunt active power filter under distorted voltage conditions», IEEE, 38th Annual Conference on Industrial Electronics Society, IECON 2012, pp: 4973–4978, 25-28 Oct. 2012.
- [16] M. Elbar, A. Kouzou and M.O. Mahmoudi. «Fuzzy controller based 3level 4wires shunt active filter for quality improvement under unbalanced conditions», The 2nd International Conference on Power Electronics and their Applications (ICPEA 2015), University of Djelfa, Algeria; 03/2015.
- [17] S. Calligaro, F. Pasut, R. Petrella, A. Pevere «Modulation Techniques for Three-Phase Three-Level NPC Inverters: a Review and a Novel Solution for Switching Losses Reduction and Optimal Neutral-Point Balancing in Photovoltaic Applications», Twenty-Eighth Annual IEEE of Applied Power Electronics Conference and Exposition (APEC), 2013, pp: 2997 – 3004.
- [18] B. Sangeetha, K. Geetha «Performance of multilevel shunt active filter for smart grid applications» Electric Power Systems and Energy Systems, vol.63, 2014, pp. 927–932
- [20] A. Chebabhi, M-K Fellah, A. Kessal, M-F Benkhoris «Fuzzy logic and Selectivity controllers for the paralleling of four-leg shunt active power filters based on Three Dimensional Space Vector Modulation», IEEE, 3rd International Conference on control, Engineering & Information Technology (CEIT), 2015.
- [21] N. Altin, O. Kaplan, S. Ozdemir, «Three-Phase Three-Level Inverter Based Shunt Active Power Filter», IEEE, 16th International Power Electronics and Motion Control Conference and Exposition, 2014, pp. 799 – 804
- [22] H-M. Nejad, S. Mohammadi, B. Farhangi, «Novel Control Method for Reducing EMI in Shunt Active Filters with Level Shifted Random Modulation», IEEE, The 6th International Power Electronics Drive Systems and Technologies Conference (PEDSTC), 2015, pp. 585 – 590